Journal of Power Sources 190 (2009) 553–557

Contents lists available at ScienceDirect

Journal of Power Sources

journal homepage: www.elsevier.com/locate/jpowsour

Short communication

Effect of carbon coating on thermal stability of natural graphite spheres used as anode materials in lithium-ion batteries

Yoon-Soo Park[a], Hyun Joo Bang[b], Seh-Min Oh[c], Yang-Kook Sun[b,**], Sung-Man Lee[a,*]

[a] Department of Advanced Materials Science and Engineering, Kangwon National University, Chuncheon Kangwon-Do 200-70, Republic of Korea
[b] Department of Chemical Engineering, Center of Information and Communication Materials, Hanyang University, Seoul 133-791, South Korea
[c] Carbonix, Inc., 938-3, Taegok-ri Buk-myeon, Jeongup-si Jeonbuk, 580-812, Republic of Korea

ARTICLE INFO

Article history:
Received 11 November 2008
Received in revised form 31 December 2008
Accepted 14 January 2009
Available online 5 February 2009

Keywords:
Lithium-ion battery
Thermal stability
Natural graphite electrode
Carbon coating

ABSTRACT

To investigate the effect of non-graphitic carbon coatings on the thermal stability of spherical natural graphite at elevated temperature, differential scanning calorimetry (DSC) and X-ray diffraction (XRD) measurements are performed. Data from DSC studies show that the thermal stability of the surface modified natural graphite electrode is improved. The surface modification results in a decrease in the BET surface specific area. An improvement in coulombic efficiency and a reduction in irreversible capacity are also observed for the carbon-coated natural graphite. X-ray diffraction analysis confirms that carbon coating alleviates the release of intercalated lithium from natural graphite at an elevated temperature and acts as a protective layer against electrolyte attack.

1. Introduction

Graphite has been widely used as an anode material for lithium-ion batteries. Recently, much attention has been directed towards natural graphite (NG) due to its low cost and intrinsically high crystallinity. Unfortunately, however, a large irreversible capacity loss related to solid electrolyte interphase (SEI) film formation during the initial cycle is still a problem for its application in high-power battery applications such as hybrid electric vehicle (HEV) and electric vehicle (EV) propulsion. The nature of the SEI film is very complicated since its components vary with the type of carbon, the functional groups on the surfaces of the carbon materials and the electrolytes used. Extensive studies have been carried out to analyze the SEI film by means of various analytical methods, which showed that the major components of the SEI film are Li_2CO_3, $ROCO_2Li$, etc. [1–3]. It is also acknowledged that the formation of the SEI film has a strong relationship with the surface area of the carbon contact with the electrolyte, even though the extent of the SEI is not linearly related to the surface area of carbon [1–3]. Therefore the BET specific surface area of carbon is a useful parameter for estimating the irreversible capacity [4–6].

Extensive research efforts have been devoted to modifying the surface of natural graphite to decrease the surface area in an attempt to reduce the irreversible capacity via mild oxidation [7], coating with pyrolytic carbon [8,9], and Li_2CO_3 [10], ionic conductive polymer [11], and partial doping with Li [12].

Surface modification by coating the graphite surface has been reported as an effective approach to suppress the irreversible intercalation of the solvated species and the side-reactions leading to the formation of the SEI layer [8,12–15]. In this regard, spherical natural graphite is more favourable than flaky natural graphite as an anode material because it can provide an improved energy density and rate capability. Accordingly, carbon-coated spherical natural graphite is considered to be a very promising anode material for lithium-ion batteries.

Recently, it was reported that the SEI film not only degraded the electrochemical properties of carbon anode materials but also initiated the thermal runway of Li-ion batteries. Several researchers have studied the thermal behaviour of graphite anodes by means of differential scanning calorimetry (DSC) [16–28] and accelerated rate calorimetry (ARC) [29–33]. The thermal stability of the anode is a critical parameter in the thermal runway of lithium-ion batteries. Exothermic reactions associated with carbonaceous anode materials are initiated with SEI layer decomposition, followed by reaction of the intercalated lithium with an electrolyte, electrolyte decomposition and a carbothermal reaction of carbon anode materials. Several publications have reported a similar reaction mechanism [23,27,28].

* Corresponding author. Tel.: +82 33 250 6266; fax: +82 33 250 6260.
** Corresponding author. Tel.: +82 2 2220 0524; fax: +82 2 2282 7329.
E-mail addresses: yksun@hanyang.ac.kr (Y.-K. Sun), smlee@kangwon.ac.kr (S.-M. Lee).

0378-7753/$ – see front matter © 2009 Elsevier B.V. All rights reserved.
doi:10.1016/j.jpowsour.2009.01.067

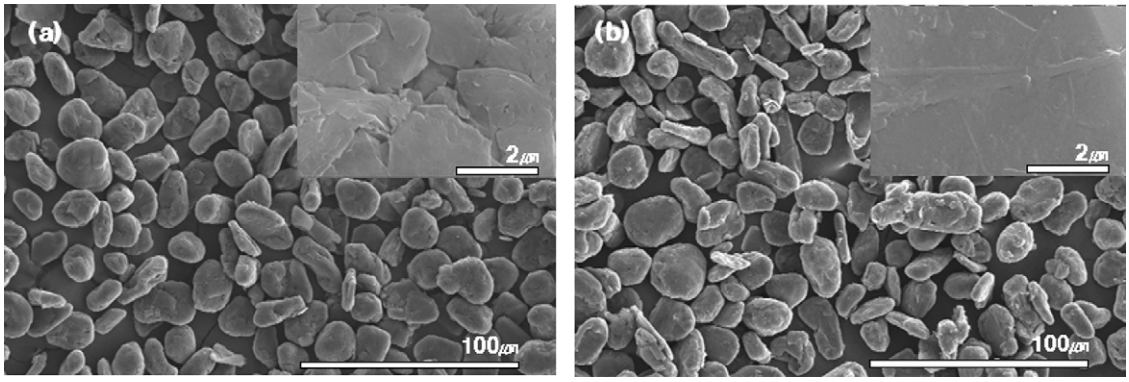

Fig. 1. FE-SEM images of (a) unmodified and (b) carbon-coated NG.

It is necessary to evaluate the thermal stability of carbon-coated natural graphite since safety is one of the main concerns for Li-ion battery application. Only a few studies have investigated the thermal stability of the carbon-coated natural graphite. The activity and the enthalpy of the exothermic reaction of the lithiated carbon anode in the presence of electrolyte/PVDF binder is dependent on the morphology and the surface chemistry of graphite, as well as on the degree of lithiation [16–19]. Yang et al. [27] compared the thermal stability of two different types of graphite and reported that carbon coating affects the heat production caused by SEI decomposition and the onset temperature for the structural collapse reaction.

In this work, the effect of carbon coating on the thermal stability of spherical natural graphite is examined using unmodified and carbon-coated natural graphite spheres of similar shape and particle size.

2. Experimental

Unmodified natural graphite and the carbon-coated natural graphite samples were used as provided by Carbonix, Inc., Korea. A proprietary coating method was utilized to prepare the carbon-coated spherical NG. Morphological analysis of the graphite samples was conducted with a scanning electron microscopy (SEM).

For electrochemical measurements, coin cells were assembled in an argon-filled glove-box with a working electrode and lithium-foil counter electrode. The working electrode was prepared by coating a slurry of graphite (90 wt.%) and poly(vinylidene fluoride) (PVDF) binder (10 wt.%) dissolved in N-methyl pyrrolidone (NMP) on a copper foil. The slurry-coated electrode was dried at 120 °C for 12 h. The electrolyte was 1 M $LiPF_6$ in a mixture of ethylene carbonate (EC) and diethyl carbonate (DEC) (1:1 by volume, provided by Techno Semichem Co., Ltd., Korea). The cells were galvanostatically cycled at 0.2 mA cm^{-2} between 0.005 and 2.0 V at 30 °C.

For DSC measurements, the cells were pre-cycled three times to reach a stable capacity level and the cycling was interrupted when the cells were charged to a fully intercalated state. The charged cells were disassembled in a glove-box. Discs with a diameter of 0.5 cm and a copper current-collector were cut from the electrode sheet without removing the electrolyte and transferred to a high-pressure stainless-steel pan with a gold-plated copper seal. The DSC scans were performed with a DSC 200 F3 instrument (NETZSCH, Germany) at various scanning rates in the range from 2.5 to 20 °C min^{-1}. The weight of each DSC pan with the sample was constant before and after DSC measurements, indicating that there was no leakage during the experiments.

Powder X-ray diffraction (XRD) with Cu K_α radiation was used to identify a lithiated state and structural characteristics of graphite electrodes as a function of temperature. The sample for XRD analysis was prepared by heating fully-lithiated samples to the designated temperature in the DSC system, followed by rapid cooling to room temperature.

3. Results and discussion

Scanning electron micrographs of the unmodified NG and the carbon-coated NG are presented in Fig. 1. Both graphite samples have similar shapes and particle sizes. It can be seen from the inset in Fig. 1(a) that the unmodified NG has rough and craggy surface, whereas the surface of the carbon-coated NG is smooth and shows no clear cracks (see the inset in Fig. 1(b)). To investigate the surface structure and confirm the existence of the coated-carbon layer on the surface of NG, Raman spectroscopy has been employed to evaluate the degree of surface disorder of the carbon materials [34,35]. Raman spectra of the unmodified and the carbon-coated NG samples are shown in Fig. 2. A pair of peaks in the range of 1200–1800 cm^{-1} is observed for both samples. The band at approximately 1580 cm^{-1} is a G-band corresponding to the E_{2g2} vibration mode in the graphitic structure of carbon materials, whereas the band at 1360 cm^{-1} (D-band) represents the A_{1g} vibration mode caused by the disordered structure in the carbon materials. The intensity ratio of the two peaks, R ($R = I_D/I_G$), can be used to estimate the degree of disorder on the surface of the unmodified NG and the carbon-coated NG. As shown in Fig. 2, the spectrum for unmodified NG exhibits a distinct G-band and a small D-band. In case of carbon-coated NG, the G-band becomes broader and smaller, and the D-band becomes broader and higher. As a result, the inten-

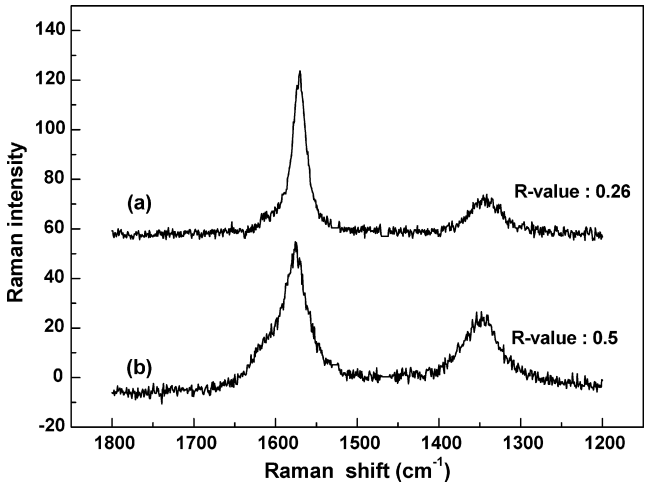

Fig. 2. Raman spectra and R-values of (a) unmodified and (b) carbon-coated NG: R-value defined as intensity ratio of two peaks ($R = I_D/I_G$).

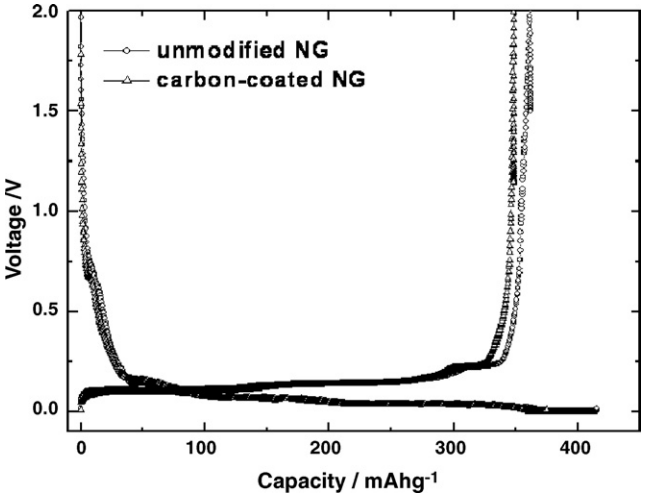

Fig. 3. Initial discharge and charge curves of (a) unmodified and (b) carbon-coated NG in voltage range of 0.005–2.0 V at current density of 0.2 mA cm^2.

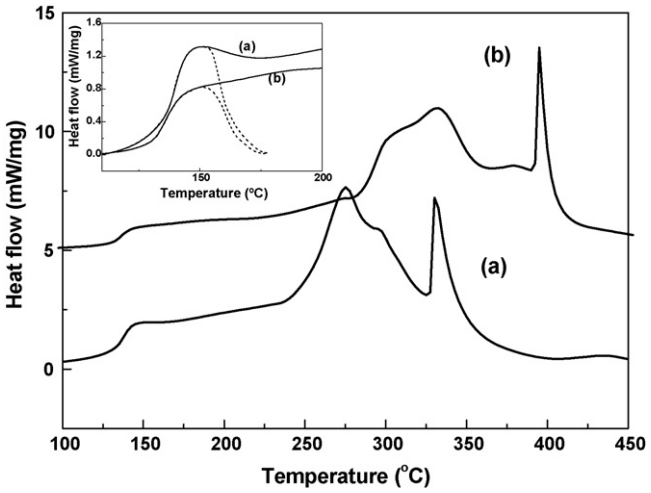

Fig. 4. DSC curves of (a) unmodified and (b) carbon-coated NG electrodes in fully-lithiated state at scan rate of 10 °C min^{-1}.

sity ratio R of the unmodified NG is 0.26 and increases to 0.5 for the carbon-coated NG. This implies that a layer of non-graphitic carbon exists on the surface of the original NG after carbon coating.

Fig. 3 shows the initial discharge and charge (intercalation and deintercalation) curves for both the unmodified NG and the carbon-coated NG in the voltage range of 0.005–2.0 V. The initial discharge capacity (intercalation) of the unmodified NG is 415 mAh g^{-1} and the charge capacity (deintercalation) is 362 mAh g^{-1}, which results in a coulombic efficiency of 87.2% on at the first cycle. The carbon-coated NG delivers 374 mAh g^{-1} of discharge capacity and 348 mAh g^{-1} of charge capacity with a coulombic efficiency of 93.0%. The reversible capacity of the carbon-coated NG slightly decreased, compared to that of the unmodified NG (362 mAh g^{-1}). However, the irreversible capacity of the carbon-coated NG drastically decreases from 54 to 26 mAh g^{-1} with improved coulombic efficiency. The enhanced coulombic efficiency and the reduced irreversible capacity of the carbon-coated NG on the first cycle can be attributed to a decrease in BET specific surface area and the existence of non-graphitic carbon on the surface structure. The measurement of the BET specific surface area for the unmodified NG shows 5.67 m^2 g^{-1}, whereas that for the carbon-coated NG is only 0.6 m^2 g^{-1}.

The DSC curves of unmodified NG and carbon-coated NG electrodes at a fully-lithiated state are given in Fig. 4. It is well known that the SEI film formed during the initial cycle at room temperature is decomposed by temperature-induced reactions, followed by continuous reformation and decomposition as a function of temperature, which is responsible for the exothermic reaction observed below approximately 225 °C on the DSC curves [24,27–30]. The DSC curve of the unmodified NG shows an exothermic reaction starting from 125 °C and then continues to 250 °C with a similar magnitude of heat generation. Two major exothermic reactions are observed after 250 °C which are related to the structural collapse of carbon material and inter-reaction with electrolyte [27]. The exothermic peak due to the initial SEI film decomposition is illustrated as the dotted line curves in the inset of Fig. 4. The estimated heat generation of the unmodified NG is 240 J g^{-1}. Surprisingly, the carbon-coated NG shows a lower heat generation of 144 J g^{-1}, which is 40% less than from the unmodified NG. Considering the reduction ratio of the irreversible capacity (0.48 = 26 mAh g^{-1}/54 mAh g^{-1}), the heat generation for the initial SEI decomposition is proportionally reduced as the initial irreversible capacity is reduced. This is consistent with the previous finding of Yang et al. [27]. This is worth noting, however, that a drastic decrease in the BET specific surface area of the carbon-coated NG does not result in the same reduction ratio of the irreversible capacity and exothermic heat generation of the initial SEI film decomposition.

It has been reported that after SEI decomposition, the reactions of the lithiated graphite with electrolyte and a fluorinated binder, such as PVDF, occur at elevated temperatures [17,24,27,30]. Moreover, these exothermic reactions might lead to the collapse of the graphite structure [27]. The consecutive reactions after SEI film decomposition result from deintercalation of the lithium in the graphite whereby Li ions diffuse from the inner structure to the surface region of the graphite particles at an elevated temperature [24,36]. To evaluate the effect of carbon coating on this phenomenon, the structural characteristics and the lithiated state of graphite electrodes as a function of temperature were examined using XRD. The XRD patterns of the unmodified NG and the carbon-coated NG electrodes heated at various temperatures are given in Fig. 5. Based on the assumption that the intensity of the XRD peaks is proportional to the amount of the phase present, it can be inferred from Fig. 5 that more lithium is extracted from the unmodified NG than from the carbon-coated NG when heated to a given temperature. For example, when the samples are heated to 300 °C, the Bragg peaks corresponding to Stage-2 (LiC_{12}) and Stage-3 still remain in the carbon-coated NG electrode, Furthermore, the peak corresponding to pure graphite phase is hardly observed. By contrast, the peak corresponding to the phase of the fully-delithiated graphite is observed in unmodified NG. In addition, the peaks for Stage-2 and Stage-3 have almost disappeared. The XRD results imply that less heat may generate at the temperature where the structural collapse occurs because intercalated Li^+ still remains in the graphite structure. The remaining lithium in the structure could, however, be detrimental if the release of intercalated lithium occurs and causes further reactions with the SEI and the other components in the electrode. To examine closely the phase variation for both samples, the intensity ratio of the peak for the Stage-1 phase (LiC_6) (I_T/I_0) as a function of temperature is presented in Fig. 6. The I_T/I_0 value was defined as the intensity ratio of the Stage-1 phase on the XRD patterns obtained at room temperature and at the designated temperatures. The peak intensity ratio of the unmodified NG electrode more rapidly decreased than that of the carbon-coated NG electrode. Therefore, it can be reasonably assumed that the carbon coating on the surface of NG suppresses the delithiation process from the inner structure to the surface of graphite at an elevated temperature.

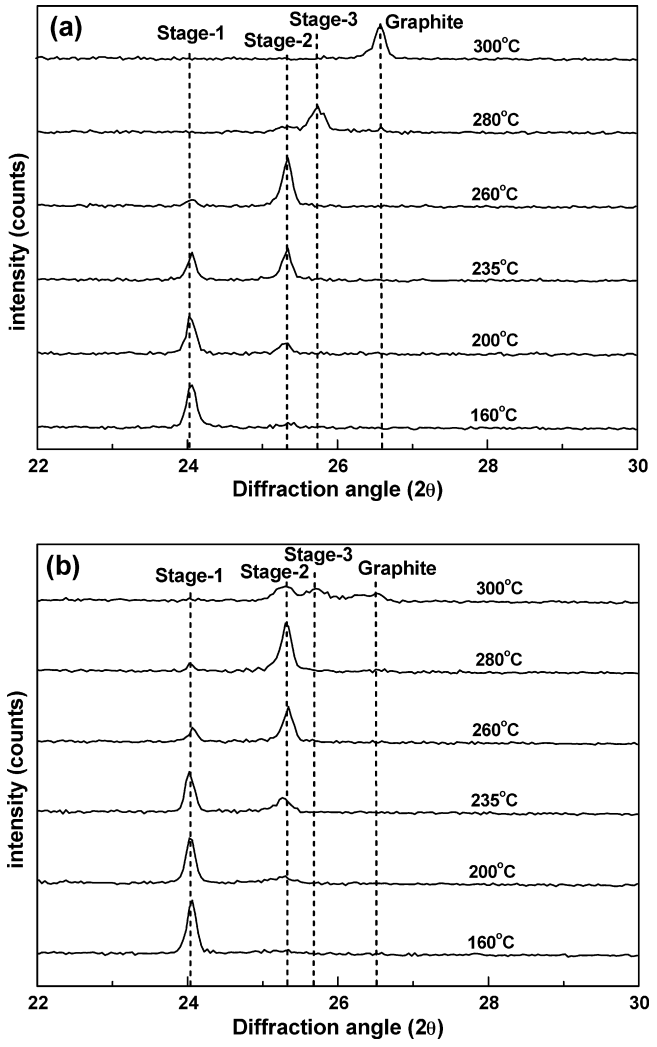

Fig. 5. XRD patterns of (a) unmodified and (b) carbon-coated NG electrodes heated to indicated temperatures.

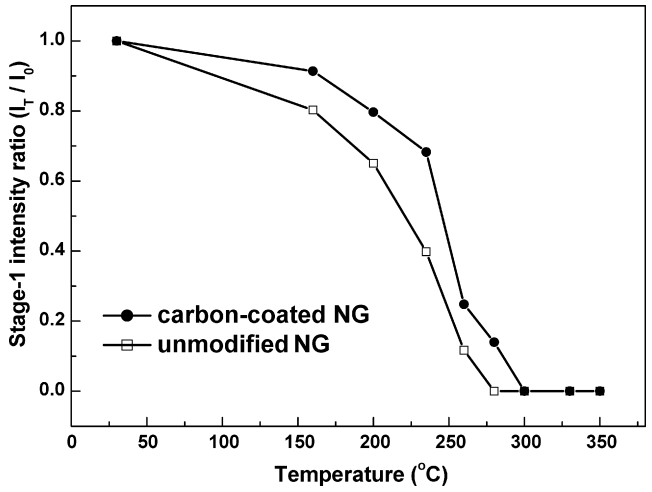

Fig. 6. Peak intensity ratio (I_T/I_0) of Stage-1 phase (LiC_6) as function of temperature: I_T/I_0 value was defined as ratio of intensity of Stage-1 phase on XRD patterns of samples heated to designated temperatures.

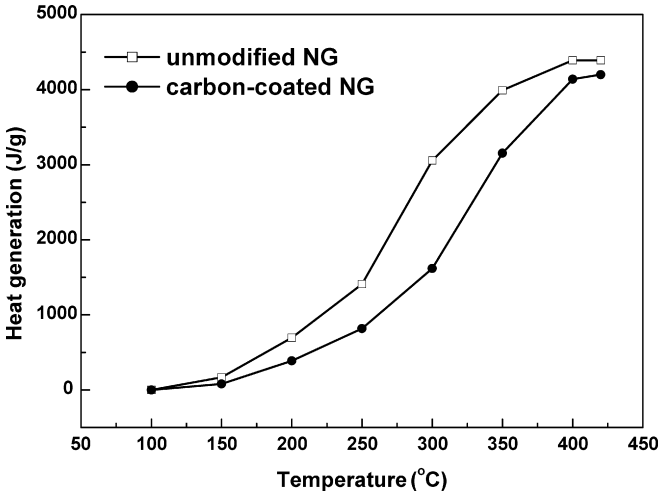

Fig. 7. Overall heat evolutions of unmodified and carbon-coated NG electrodes in fully-lithiated state as function of temperature.

Fig. 7 shows the comparison of the heat generation of both samples calculated from the DSC curves as a function of temperature. As assumed above, mild deintercalation of the carbon-coated NG at elevated temperatures leads to a lower heat evolution than that of the unmodified NG. It can be inferred that the carbon-coated NG has better thermal stability than the unmodified NG. This is consistent with results reported by Lee et al. [15] in which the less capacity

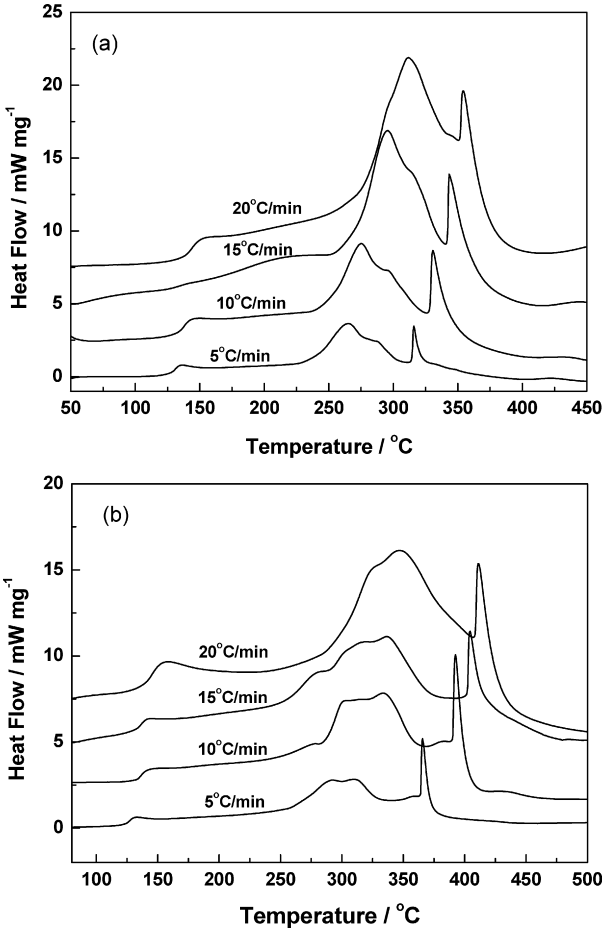

Fig. 8. DSC curves of (a) unmodified and (b) carbon-coated NG electrodes in fully-lithiated state at different scan rates from 5, 10, 15 and 20 °C min^{-1}.

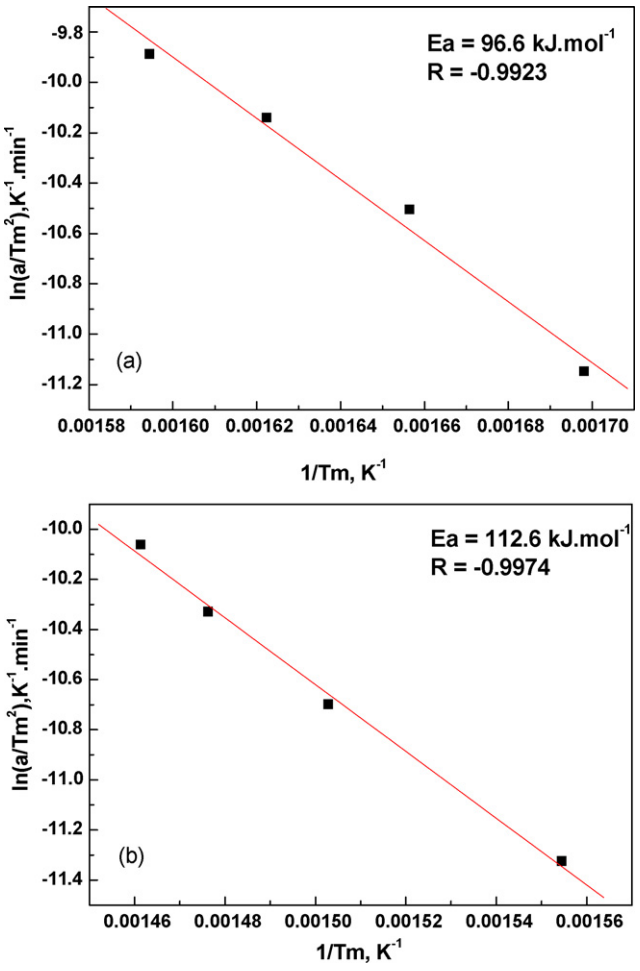

Fig. 9. Arrhenius plots of (a) unmodified and (b) carbon-coated NG electrodes.

loss after storage at an elevated temperature was observed for the fully-lithiated carbon-coated graphite than an untreated graphite electrode.

As shown in Fig. 4, a sharp exothermic peak was detected at 330 and 392 °C for the unmodified NG and carbon-coated NG sample, respectively, which was attributed to the collapse of the graphite structure [27]. A possible reaction mechanism for the sharp exothermic peak is that EC and $LiPF_6$ may have entered between the graphite sheets and reacted with the intercalated lithium to form lithium carbonate, that, in turn, results in the exfoliation of graphite [2,37]. Consequently, the lithium-ions released as a result of the structural collapse react with the PVDF binder and the remaining electrolyte to form producing by-products [27,28]. Surface modification by coating with a non-graphitic carbon layer suppresses the release of the intercalated lithium from the graphite and also protects the graphite structure from electrolyte attack. Therefore, it can be expected that the structural collapse reaction for the carbon-coated NG electrodes will be delayed to a higher temperature.

The activation energies associated with the structural collapse reaction for the unmodified NG and the carbon-coated NG were determined by performing several DSC scans at different rates. Fig. 8 shows the DSC traces of both unmodified and carbon-coated NG at different scan rates. It can be observed that as the scan rate increases, the sharp exothermic peak moves to a higher temperature with an increase in intensity. The activation energy for the structural collapse reaction was calculated by the Kissinger method [38] from DSC curves and is presented in Fig. 9. The carbon-coated NG sample shows higher activation energy than the unmodified NG sample for the structural collapse reaction. This supports the conclusion that a carbon coating on NG improves the thermal stability of unmodified NG.

4. Conclusions

Carbon-coated natural graphite shows less irreversible capacity and improved coulombic efficiency than unmodified natural graphite. The BET specific surface area of unmodified NG drastically decreases after carbon coating. The DSC study reveals that surface modification by coating with a non-graphitic carbon layer on natural graphite improves the thermal stability of spherical natural graphite. It is confirmed by XRD analysis that the carbon coating layer suppresses the release of intercalated lithium from NG at high temperatures and protects the graphite structure from electrolyte attack.

Acknowledgments

This work was supported by the Division of Advanced Batteries in the NGE Program (Project No. 10028960).

References

[1] A. Naji, J. Ghanbaja, B. Humbert, P. Willmann, D. Billaud, J. Power Sources 63 (1996) 33.
[2] D. Aurbach, A. Zaban, Y. Ein-Eli, I. Weissman, O. Chusid, B. Markovsky, J. Power Sources 68 (1997) 91.
[3] K. Kanamura, H. Tamura, S. Shiraishi, Z. Takehara, J. Electroanal. Chem. 394 (1995) 49.
[4] R. Fong, U. Von Sacken, J.R. Dahn, J. Electrochem. Soc. 137 (1990) 2009.
[5] B. Simon, S. Flandrois, A. Fevrier-Bouvier, P. Biensan, Mol. Cryst. Liq. Cryst. 310 (1998) 333.
[6] M. Winter, P. Novak, J. Monnier, J. Electrochem. Soc. 145 (1998) 428.
[7] C. Menachem, E. Pelad, L. Buretein, Y. Rosenberg, J. Power Sources 68 (1997) 277.
[8] M. Yoshio, H. Wang, K. Fukuda, Y. Hara, Y. Adachi, J. Electrochem. Soc. 147 (2000) 1245.
[9] H.-L. Zhang, S.-H. Liu, F. Li, S. Bai, C. Liu, J. Tan, H.-M. Cheng, Carbon 44 (2006) 2212.
[10] S.S. Zhang, K. Xu, T.R. Zow, Electrochem. Comm. 5 (2003) 979–982.
[11] Q. Pan, K. Guo, L. Wang, S. Fang, J. Electrochem. Soc. 149 (2002) A1218.
[12] Y.-T. Lee, C.S. Yoon, J. Prakash, Y.-K Sun, J. Electrochem. Soc. 151 (2004) A1728.
[13] I. Kuribayashi, M. Yokoyama, M. Yamashita, J. Power Sources 54 (1995) 1.
[14] W. Qiu, Q. Zhang, S. Lu, Q. Liu, Solid State Ionics 121 (1999) 73.
[15] H.Y. Lee, J.K. Baek, S.W. Jang, S.M. Lee, S.T. Hong, K.Y. Lee, M.H. Kim, J. Power Sources 101 (2001) 206.
[16] K. Edstrom, A.M. Andersson, A. Bishop, L. Fransson, J. Lindgren, A. Hussenius, J. Power Sources 97–98 (2001) 87.
[17] A.D. Pasquier, F. Disma, T. Bowmer, A.S. Gozdz, G. Amatucci, J.M. Tarascon, J. Electrochem. Soc. 145 (1998) 472.
[18] A.M. Andersson, K. Edstrom, N. Rao, A. Wendsjo, J. Power Sources 81–82 (1999) 286.
[19] F. Joho, P. Novak, M.E. Spahr, J. Electrochem. Soc. 149 (2002) A1020.
[20] J. Yamaki, Y. Baba, N. Katayama, H. Takatsuji, M. Egashira, S. Okada, J. Power Sources 119–121 (2003) 81.
[21] R. Spotnitz, J. Franklin, J. Power Sources 113 (2003) 81.
[22] H. Maleki, G. Deng, I.K. Haller, A. Anani, J.N. Howard, J. Electrochem. Soc. 147 (2000) 4470.
[23] E.P. Roth, D.H. Doughty, J. Franklin, J. Power Sources 134 (2004) 222.
[24] H.H. Lee, C.C. Wan, Y.Y. Wang, J. Electrochem. Soc. 151 (2004) A542.
[25] J. Yamaki, H. Takatsuji, T. Kawamura, M. Egashira, Solid State Ionics 148 (2002) 241.
[26] M. Holzapfel, P. Alloin, R. Yazami, Electrochim. Acta 49 (2004) 581.
[27] H. Yang, H. Bang, K. Amine, J. Prakash, J. Electrochem. Soc. 152 (2005) A73.
[28] Q. Wang, J. Sun, X. Yao, C. Chen, J. Electrochem. Soc. 153 (2006) A329.
[29] M.N. Richard, J.R. Dahn, J. Electrochem. Soc. 83 (1999) 71.
[30] M.N. Richard, J.R. Dahn, J. Electrochem. Soc. 146 (1999) 2068.
[31] M.N. Richard, J.R. Dahn, J. Electrochem. Soc. 146 (1999) 2078.
[32] D.D. MacNeil, D. Larcher, J.R. Dahn, J. Electrochem. Soc. 146 (1999) 3596.
[33] J. Jiang, J.R. Dahn, Electrochem. Solid-State Lett. 6 (2003) A180.
[34] K. Suzuki, T. Hamada, T. Sugiura, J. Electrochem. Soc. 146 (1999) 890.
[35] T. Tsumura, A. Katanosaka, I. Souma, T. Ono, Y. Aihara, J. Kuratoni, M. Inagaki, Solid State Ionics 135 (2000) 209.
[36] A.M. Andersson, K. Edstrom, J. Electrochem. Soc. 148 (2001) A1100.
[37] G.C. Chung, H.S. Kim, S.I. Yu, S.H. Jun, J.W. Choi, M.H. Kim, J. Electrochem. Soc. 147 (2000) 4341.
[38] H.E. Kissinger, Anal. Chem. 29 (1957) 1702.